INFLUENCE OF IRON NANOPARTICLES ON THE SHAPE MEMORY EFFECT OF PVA

*Anette Lang[1], Alexandru Sover[1]**
[1]University of Applied Sciences Ansbach, Germany
*Emails: anette.lang@hs-ansbach.de , *a.sover@hs-ansbach.de*

Abstract - Shape memory polymers (SMP) can be used in numerous applications, for example in medical engineering, control technology, or in the automotive industry. Various triggers can be used to "remember" a programmed shape, such as temperature, pH value, humidity or light.
One example of SMP is polyvinyl alcohol (PVA), which is characterised by biocompatibility, high hydrophilicity and non-toxicity as well as efficient shape memory behaviour. PVA reacts to the stimulus of temperature.
In this work, the influence of incorporated nanoparticles on the shape memory effect of PVA will be investigated. For this purpose, the glass transition temperature of PVA containing different iron nanoparticles is determined and compared by means of Differential Scanning Calorimetry (DSC). In addition to the impact of the integrated nanoparticles on the switching temperature, consideration is also given to the quality of the resetting characteristics linked with the shape memory effect. These studies employ thermomechanical analysis as a tool to gain insights into this phenomenon.
The inclusion of iron nanoparticles has been observed to result in a slight alteration of the switching temperature, while significantly influencing the shape memory effect and reducing the strain recovery rate by approximately 15%. The strain fixity rate simultaneously increases by approximately 50%. However, the size and structure of the iron nanoparticles showed no discernible impact on the observed phenomenon.

Keywords: Shape memory polymers, Nanoparticles, Switching temperature, Strain recovery rate, Strain fixity rate, TMA measurement.

1. Introduction

Shape memory polymers are polymers that exhibit the capacity to retain a programmed shape in response to a specific stimulus. In consequence, these polymers can perform a movement. A variety of stimuli may be employed, including temperature, pH, humidity and solvents, among others. [5,9] This research aims to examine the shape memory effect (SME) of polyvinyl alcohol (PVA) in connection with iron nanoparticles focusing on the impact of the iron nanoparticles on the switching temperature and the shape memory effect depending on their dimensions and shell structure.

In addition to its SME, PVA has good biocompatibility features which, in combination with its use as a 3D printing material for fused deposition modelling, can lead to a suitable 4-D drug delivery system. [8]

Regarding the molecular weight of PVA, the PVA composites created by including nanomaterials also induce alterations in the mechanical properties and SME. [1,2] So the integration of silver nanoparticles has already demonstrated a positive effect on the SME of PVA. [3] Furthermore, the incorporation of graphite nano-fillers into the PVA matrix resulted in the fabrication of shape memory nanocomposites with augmented performance characteristics. [4] The objective of this study is to investigate the influence of iron nanoparticles of varying sizes and shells on the SME of PVA. Given the magnetic properties of iron, it is hypothesised that this will enable non-contact heating and thus the triggering of the SME of PVA at a short distance. [10]

The shape memory effect is not contingent on a singular material attribute of individual polymers; rather, it is the consequence of a multifaceted interplay of numerous variables. These encompass the polymer structure, the polymer morphology, and

https://doi.org/10.17683/ijomam/issue19

the processing and programming technology employed. [9]

In particular, the structures of SMPs, whose stimulus is temperature, are composed of hard and soft segments. The hard segments comprise chemical (or physical) cross-linking points and crystalline regions (or stiffness chains), which collectively determine the permanent shape of the polymer chain network. The soft segments of the SMP are constituted by crystalline areas. The crystallinity of the soft segments is dependent on temperature, as is their morphology. Upon reaching the glass transition temperature (Tg), the soft segments of these SMPs can undergo deformation in length and orientation, allowing the SMPs to be fixed in a temporary shape following cooling below Tg. This process minimises the elongation of the SMPs. In this case, the strain energy is stored within the polymer chain network. Upon reheating, the deformed polymer chains regain their mobility, resulting in the release of the stored energy. Consequently, the SMP reverts to its original configuration, which is retained by the hard segment.[4]

The shape memory effect can be quantified in cyclic thermomechanical tests. A single cycle comprises two distinct phases: the programming of the test specimen and the restoration of its permanent shape.

In the initial phase, the specimen is heated to a temperature above its switching temperature and stretched to a maximum strain. At constant elongation, the specimen is then cooled below the switching temperature to fix the temporary shape. After heating to a temperature above the switching temperature, the sample contracts and the permanent shape is restored. The measuring cycle then commences anew.

The strain recovery ratio R_r is a quantitative measure of the material's ability to store its permanent shape and indicates the extent to which a real strain that occurred during programming is reversed in the subsequent shape memory transition.

The total strain recovery ratio ($R_{r,tot}$) is defined as the strain recovery following N cycles relative to the initial shape of the specimen.

The following formula for $R_{r,tot}$ was used to calculate the total strain recovery rate after two cycles (N=2):

$$R_{r,tot}(N) = \frac{\varepsilon_m - \varepsilon_p(N)}{\varepsilon_m} \quad (1)$$

In the context of this study, the term "ε_m" is used to denote the strain above the switching temperature, which is employed for the purpose of programming the new shape. In contrast, the term "ε_p" is used to denote the permanent strain, which is applied after the memorisation of the permanent shape.

In addition to the strain recovery rate $R_{r,tot}$, the strain fixity rate R_f is also employed for evaluation purposes in this study. The strain fixity rate R_f characterises the capacity of the switching segment to sustain the mechanical deformation that was applied during programming. Consequently, it indicates the precision with which the sample can be fixed in this position after deformation to ε_m. The resulting transient shape invariably deviates from the shape achieved by deformation.

$$R_f(N) = \frac{\varepsilon_u(N)}{\varepsilon_m} \quad (2)$$

The term "ε_u" is used to describe the elongation observed in a stress-free state after the programming process. [6]

2. Materials and Methods

The PVA (KURARAY POVAL™, type 4-98) was acquired from Kuraray Europe GmbH.

The two nanoparticles were kindly provided by SEON (University Hospital Erlangen, Section of Experimental Oncology and Nanomedicine (SEON). The structure of the nanoparticles differs in terms of size and the composition of their shells as well.

$SEON^{Dex}$ is composed of dextran-coated iron oxide nanoparticles dispersed in water, with an iron concentration of 25.82 ± 0.15 mg/mL and a mean hydrodynamic size of 29 nm. The lauric acid-loaded ferrofluid, also dispersed in water, has an iron content of 4.57 mg/mL and a mean hydrodynamic size of 191 nm.

Films were produced for the analytical tests on polyvinyl alcohol (PVA). A solution with a concentration of 10 %wt. was prepared using demineralised water and stirred at a temperature of 70 °C for a period of one hour. Subsequently, the solution was levelled and dried in a drying oven at 50 °C for one hour, resulting in a film thickness of 40 µm. The film with nanoparticles was produced in the same manner, with the exception that only 10 % of the demineralised water was replaced with the nanoparticle solution when the initial solution was prepared. An overview of the films tested is provided in Table 1.

Table 1: Description of the samples

Sample	Concentration nanoparticle solution [wt%]	Concentration PVA [wt%]
Pure PVA	--	100
PVA-film	--	10
PVA-film with $SEON^{Dex}$	10	10
PVA-film with lauric acid-loaded ferrofluid	10	10

The glass transition temperatures of the films were determined by differential scanning calorimetry (DSC). This is a common method to characterize the glass transition temperature and thus the switching temperature of the SMP. [11] The measurements were carried out using the DSC3+ from Mettler Toledo. The temperature range was set to 25 °C to 220 °C, with a heating rate of 10 K/min. Each measurement comprised two heating runs and one cooling run with a cooling rate of -10 K/min. The second heating run was employed for evaluation purposes, with the aim of excluding effects from the previous history of the material. This approach ensures that only the modified material properties resulting from the interaction of the nanoparticles with the soft segment of the PVA are determined.

To investigate the SME, the strain recovery rate $R_{r,tot}$ and the strain fixity rate R_f of PVA with and without the nanoparticles were measured. This was achieved by employing a corresponding method utilising thermomechanical analysis (TMA). As demonstrated in prior studies, TMA is a viable method for determining the aforementioned characteristic values. [7] All thermomechanical analyses were carried out using the TMA2+ device, manufactured by Mettler Toledo. The resulting TMA samples, along with their respective installations within the TMA device, are illustrated in Figure 1. The method is illustrated in the force-temperature diagram (see diagram 1), with each sample undergoing the cycle twice starting at step 1.

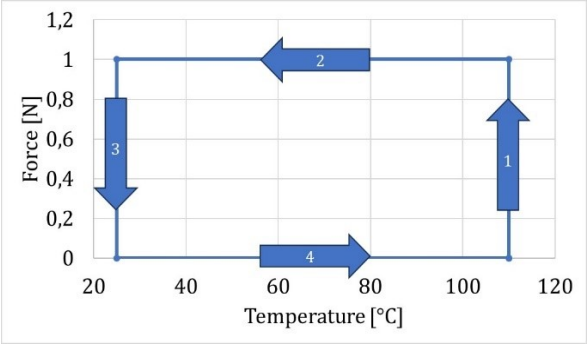

Figure 1: Force-temperature-diagram

As shown in the diagram of figure 1, the sample is heated to 110°C and then a force of 1 N is applied. The resulting change in length is documented. The sample is then cooled to 25°C under the load of 1 N before being released. The sample is then reheated to 110 °C without force while the change in length is being measured. This cycle is then repeated a second time. Figure 2 shows the samples and the sample position inside the testing equipment.

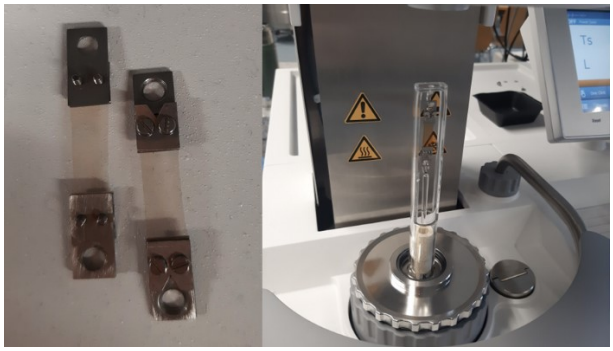

Figure 2: TMA sample on the left, sample inserted in the TMA device on the right.

3. Results and Discussion

3.1 Influence on the Switching Temperature

Figure 3 illustrates the DSC curves for the analysed samples within the essential temperature range of 30 to 120 °C.

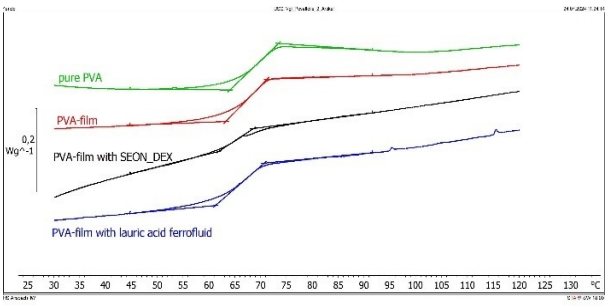

Figure 3: DSC curves in the temperature range of 30 - 120 °C

All samples exhibited a distinct step in the baseline of the measurement curve. This step showed a slight displacement at low temperatures from pure PVA to the PVA film containing the nanoparticles. The Tg was determined in accordance with the DIN ISO11357 standard. An overview of the measured Tg values is presented in Table 2.

Table 2: Measured glass transition temperatures Tg

Sample	Tg [°C]
Pure PVA	68,8 °C
PVA-film	67,1 °C
PVA-film with SEON^{Dex}	65,6 °C
PVA-film with lauric acid-loaded ferrofluid	65,8 °C

The production of a PVA film from a 10 wt% solution resulted in a reduction of the Tg by approximately 1.5 K, with a final value of 67.1 °C. The addition of the nanoparticles caused a further shift of the Tg by 1.5 K, which led to a reduction of 3 K in the Tg of pure PVA. A comparison of the two nanoparticles revealed no significant difference, despite the nanoparticles differing in both diameter and shell structure.

The glass transition temperature of PVA with nanoparticles shifts to slightly lower temperatures, which has a negligible effect on the bonds of the soft segment, thus on the polymer structure. To make a more precise statement regarding the nature of the influence, further comprehensive investigations are being required. The impact of the nanoparticle content is also a subject of interest, given its abillity to influence the heating rate during contactless heating via magnetism. This is a critical aspect for the SME of PVA and the development of potential drug delivery systems.

3.2 Influence on the Strain Recovery Rate $R_{r,tot}$ and the Strain Fixity Rate R_f

Figure 4 illustrates the TMA measurement for the PVA film (PVA film with SEON^{DEX} and PVA film with lauric acid-loaded ferrofluid). It is notable that the sample displays a greater elongation under the same force application. The integration of the nanoparticles causes an increase of the elongation from approximately 20% to approximately 60% and 75%, respectively.

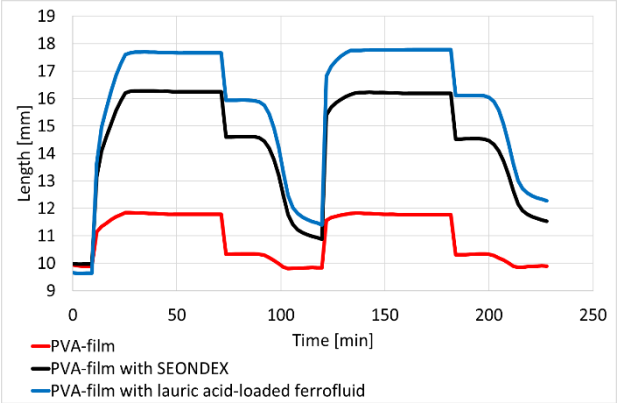

Figure 4: TMA measurement for PVA-film, PVA-film with SEON^{DEX} and PVA-film with lauric acid-loaded ferrofluid

The pure PVA film has a very good strain recovery rate in the two cycles measured. Here, 100% is achieved and the PVA film returns to its original shape. The films with iron nanoparticles show a different behaviour reducing the elongation recovery by 13 % and 16 % respectively (see Table 3).

Table 3: Strain recovery rate

Sample	$R_{r,tot}$(N=2) [%]
PVA-film	100
PVA-film with SEON^{Dex}	87
PVA-film with lauric acid-loaded ferrofluid	84

It is of interest to note that the specific type of iron nanoparticles does not have a significant impact on the strain recovery rate. The discrepancy in elongation recovery between the two films with nanoparticles is considerably less pronounced in comparison to the pure PVA film.
The integration of the nanoparticles into the PVA also resulted in an increase in the strain fixity rate R_f of approximately 50 % after two cycles. Furthermore, there was no significant difference in the influence on the strain fixity rate between the two used nanoparticle types (see Table 4).

Table 4: Strain fixity rate

Sample	R_f(N=2) [%]
PVA-film	23
PVA-film with SEON^{Dex}	71
PVA-film with lauric acid-loaded ferrofluid	77

A detailed examination of the two characteristic values $R_{r,tot}$ and R_f reveals that the nanoparticles exert a discernible impact on both the hard and soft segments of the PVA. While there is a notable decline of the strain recovery rate, the strain fixity rate presents a strikingly deviant trend. The extent to which these two characteristic values can be controlled by an increase in the iron particle concentration remains to be assessed through further investigations.

4. Conclusions

The effect of adding iron nanoparticles on the switching temperature of PVA films, determined by measuring the Tg, is negligible. The Tg only shifts to lower temperatures by up to 3 K, irrespective of the type of nanoparticles included.

As shown by the strain recovery rate, the iron nanoparticles have a significant influence on the ability of the SMP-PVA to maintain its permanent shape. The situation is different for the strain fixity rate. Here the nanoparticles involve a significant improvement meaning that the SMP-PVA can retain its new shape better. The underlying mechanism needs further investigation. However, the nanoparticles clearly modulate the chemical and physical cross-linking points and crystalline regions.

The knowledge gained may be helpful for applications in the medical field, for example, particularly in the context of drug delivery. As the switching temperature has changed only slightly, the desired switching property regarding the temperature remains unchanged. A positive aspect is the change of the strain fixity rate, whose increase means that special requirements on the drug delivery shape can be better represented form. The water solubility of PVA should also be highlighted. Here, two trigger points can be combined during drug delivery - shape change due to the SME and detachment due to water.

Acknowledgements

The authors would like to express their gratitude to SEON (Section for Experimental Oncology and Nanomedicine) of the University Hospital Erlangen for providing the iron nanoparticles.

References

[1] Alfayyadh, A. A., Lotfy, S., Basfar, A. A., & Khalil, M. I. (2017). Influences of poly (vinyl alcohol) molecular weight and carbon nanotubes on radiation crosslinking shape memory polymers. Progress in Natural Science: Materials International, 27(3), 316-325.

[2] Bhanushali, H., Amrutkar, S., Mestry, S., & Mhaske, S. T. (2022). Shape memory polymer nanocomposite: a review on structure–property relationship. Polymer Bulletin, 79(6), 3437-3493.

[3] Canbay, C. A., & Ünlü, N. (2021). Production and characterization of shape memory polymeric nanocomposite materials. Journal of Molecular Structure, 1227, 129708.

[4] Du F.-P., Ye E.-Z., Tang C.-Y., Ng S.-P., Zhou X.-P., Xie X.-L. (2012). Microstructure and Shape Memory Effect of Acidic Carbon Nanotubes Reinforced Polyvinyl Alcohol Nanocomposites, J. APPL. POLYM. SCI. 2013, DOI: 10.1002/APP.38807

[5] Du, H., & Zhang, J. (2010). Solvent induced shape recovery of shape memory polymer based on chemically cross-linked poly (vinyl alcohol). Soft Matter, 6(14), 3370-3376.

[6] Lendlein, A., & Kelch, S. (2002). Shape-memory polymers. Angewandte Chemie International Edition, 41(12), 2034-2057.

[7] Lu, J., Arsalan, A., Dong, Y., Zhu, Y., Qian, C., Wang, R., ... & Ali, K. N. (2017). Shape memory effect and recovery stress property of carbon nanotube/waterborne epoxy nanocomposites investigated via TMA. Polymer Testing, 59, 462-469.

[8] Melocchi, A., Inverardi, N., Uboldi, M., Baldi, F., Maroni, A., Pandini, S., ... & Gazzaniga, A. (2019). Retentive device for intravesical drug delivery based on water-induced shape memory response of poly (vinyl alcohol): design concept and 4D printing feasibility. International journal of pharmaceutics, 559, 299-311.

[9] Moreno-Marcelino, J. E., Gutierrez-Segura, E., Vilchis-Nestor, A. R., Castro-Longoria, E., & Lopez-Tellez, G. (2020). Shape memory hybrid based on polyvinyl alcohol and 0D silver nanoparticles. Polymer Testing, 90, 106668.

[10] Namathoti, S., & PS, R. S. (2022). A review on progress in magnetic, microwave, ultrasonic responsive Shape-memory polymer composites. Materials Today: Proceedings, 56, 1182-1191.

[11] Wagermaier, W., Kratz, K., Heuchel, M., & Lendlein, A. (2010). Characterization methods for shape-memory polymers. Shape-memory polymers, 97-145.